COMMUNICATION

Biomimetic Surface Coatings for Atmospheric Water Capture Prepared by Dewetting of Polymer Films

Stuart C. Thickett, Chiara Neto, and Andrew T. Harris**

Harvesting water directly from the atmosphere is an increasingly popular, alternative method of collecting drinking water. Throughout South and Central America, *FogQuest*[1] utilizes large sheets of a fine mesh-like material to trap water from fog and mist; this approach has been successful in many rural communities. Herein, we demonstrate the synthesis of micropatterned surface coatings that capture water from a humid atmosphere in the absence of a fog or mist when cooled below the surface dew point. The micropatterns are both topographical and chemical in character and mimic a mechanism observed in nature.[2] The coatings are prepared by the dewetting of thin polymer bilayer films on solid substrates[3] to create a surface consisting of raised hydrophilic bumps on a hydrophobic background, which allow for an enhanced rate of surface water condensation relative to flat films under representative climatic conditions. These surfaces could readily be made on a large scale and be integrated with the existing building infrastructure to help meet the water demands of a growing global population, as well as facilitate access to a stable supply of drinking water in remote areas.

Our inspiration for atmospheric water collection comes from the *Stenocara* beetle, a native of the Namib Desert in southwest Africa. The Namib Desert is one of the driest environments in the world[4] with minimal ground water: the only reliable source of water is fog-laden winds from the Atlantic Ocean. The *Stenocara* has a unique exoskeleton that allows it to survive in this environment,[2] consisting of an array of raised hydrophilic bumps approximately 0.5–1.5 mm apart and 0.5 mm in diameter, on a hydrophobic background. This structured surface allows for efficient condensation of water from the air; water condenses on the hydrophilic bumps when the surface is cooler than the surrounding air, forming droplets that grow in size yet are pinned to their location due to the very hydrophobic exoskeleton background. These droplets grow until they detach and roll off the surface and into the mouth of the *Stenocara*, providing a reliable supply of drinking water. *Stenocara* has been described as "nature's version of a dropwise condensing surface," implying that the surface is able to undergo "direct and preferential heterogeneous vapor-to-liquid nucleation."[5] This is due to the vastly greater droplet nucleation rate on hydrophilic surfaces compared to hydrophobic surfaces, on the order of 10^{129}.[5] In the *Stenocara* beetle, the size and density of the raised hydrophilic bumps provide a good balance between water droplet detachment from the surface while minimizing re-evaporation to the atmosphere.[2,6] The available design envelope for such a hydrophilic/hydrophobic surface can be estimated by determining both the minimum and maximum theoretically stable droplet sizes on a cooled surface;[7] these have diameters of ≈1.6 μm and ≈1.5 mm, respectively, under typical atmospheric water capture conditions.

There have been numerous attempts to mimic the unique water capture mechanism of the *Stenocara* by preparing surfaces that promote atmospheric condensation. Previous strategies include the synthesis of "perfectly hydrophobic" nanofibers,[8] selective deposition of polyelectrolytes onto a hydrophobic surface,[9] patterning a perfluorinated surface with UV radiation,[6a] as well as plasma-chemical treatment.[6b] The success of these surfaces in enhancing atmospheric water capture is counteracted by their complicated synthetic procedures and the need for specialist synthesis equipment. As an alternative we present a method of creating micropatterned surfaces with regions of chemical and topographical contrast using the spontaneous dewetting of bilayers of thin polymer films. The resulting surface collects significantly more atmospheric water than a corresponding flat film, combined with improved water droplet detachment. Such coatings can be prepared on substrates of any shape using conventional techniques such as spin-coating, dip coating, or spraying, they are made from low-cost and common polymers, and the procedure is readily scalable, allowing for fabrication on the meter scale.

Dewetting is the process by which unstable thin (≈100 nm) liquid films spontaneously break apart on a substrate, driven by unfavorable intermolecular forces at the interface between the two materials.[3,10] The unstable film breaks apart into holes that grow with time, eventually transforming the film into a series of isolated droplets. Above its glass transition temperature T_g, an unstable thin polymer film on a solid substrate spontaneously undergoes morphological transformation via dewetting. When the polymer film is cooled below T_g, the resultant pattern is "frozen in," preserving the droplet morphology. We have exploited the resultant pattern to create biomimetic surfaces, whereby the dewetted polymer droplets mimic the hydrophilic bumps on the *Stenocara* exoskeleton. To create a final surface with wettability contrast between the droplet phase and the background, we investigated the dewetting of an immiscible polymer bilayer, consisting of a hydrophilic polymer layer on top of a hydrophobic polymer underlayer (**Figure 1**).

Dr. S. C. Thickett, Dr. C. Neto
School of Chemistry F11
The University of Sydney
NSW Australia 2006
E-mail: chiara.neto@sydney.edu.au
Prof. A. T. Harris
School of Chemical and Biomolecular Engineering J01
The University of Sydney
NSW Australia 2006
E-mail: andrew.harris@sydney.edu.au

DOI: 10.1002/adma.201100290

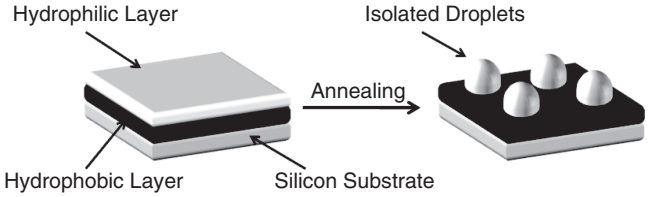

Figure 1. Proposed formation of micropatterned surfaces via the dewetting of polymer bilayer films. The top layer is an unstable P4VP film, which spontaneously dewets on the bottom PS layer.

The ability of a liquid to wet a solid surface is described by the spreading coefficient S, given by:[11]

$$S = \gamma_{solid} - (\gamma_{liq} + \gamma_{solid/liq}) \quad (1)$$

where γ_{solid} and γ_{liq} are the surface tensions of the solid and liquid and $\gamma_{solid/liq}$ is the interfacial tension of the solid/liquid interface. If $S < 0$, the liquid will spontaneously dewet from the solid substrate, allowing materials to be chosen based on their surface and interfacial tensions. Consequently, we prepared polymer bilayer films consisting of a bottom layer of polystyrene (PS) and a top layer of poly(4-vinylpyridine) (P4VP), as above the glass transition temperature of both polymers, S is strongly negative[12] (≈ -31 mN m^{-1}) and the P4VP layer will readily dewet. PS and P4VP are structurally similar but possess very different hydrophobicities; the average equilibrium water contact angle on flat PS and P4VP films were measured to be 91.3° ± 1.8° and 36.0° ± 2.7°, respectively. The hydrophilicity of P4VP is due to hydrogen bonding between water and the lone electron pair on the nitrogen atom in the P4VP monomer unit.[13]

Polymer bilayers were prepared on clean, smooth silicon substrates consisting of a PS underlayer and a P4VP top layer by sequential spin coating. Both layers were smooth, with root mean square (RMS) roughness values less than 0.5 nm measured by atomic force microscopy (AFM). Annealing was performed above 160 °C (above T_g for both polymers), and the dewetting of the P4VP layer was tracked by optical microscopy. The resultant surface morphology (which could be attained in as little as 30 s at 200 °C) consisted of a series of isolated droplets and interconnected cylinders of P4VP on a PS background (**Figure 2**). The complete dewetting of the P4VP film was only possible when the melt viscosity of the P4VP was significantly lower than that of the PS.[12] The chemical nature of the surface features was confirmed by AFM imaging before and after exposure to selective solvents for each polymer.[12] The average P4VP droplet density was 3.1 (± 1.0) × 10^3 per mm^2, while the average P4VP droplet diameter D_d displayed a weak power law dependence on the P4VP layer thickness H ($D_d \approx H^{0.18 \pm 0.02}$) (see Figure SI.1 and SI.2 in the Supporting Information); droplet diameters measured on the substrates were around 7–12 μm based on P4VP layer thicknesses used (10–110 nm). This power law dependence is weaker than the $D_d \approx H^{1.5}$ relation predicted by Sharma and Reiter[14] for single polymer layers on solid substrates, probably due to the deformation of the polystyrene underlayer upon dewetting.[12]

The droplet height and density could be controlled by pre-annealing the bilayer, below T_g of both layers (e.g., 90 °C), prior to dewetting. Pre-annealing relaxes residual stresses in the film caused by spin-coating,[3b] which in turn reduces the number of nucleation sites for dewetting. Extensive pre-annealing (>50 h) halved the final droplet density and achieved droplets approximately 13 μm in diameter. With raised hydrophilic "bumps" on a hydrophobic background phase, the surfaces are therefore microscale polymeric mimics of the *Stenocara* exoskeleton. The surfaces consist of many thousands of hydrophilic bumps per square millimetrer, a far greater number density than in *Stenocara*, but with a similar hydrophilic/hydrophobic surface area ratio.

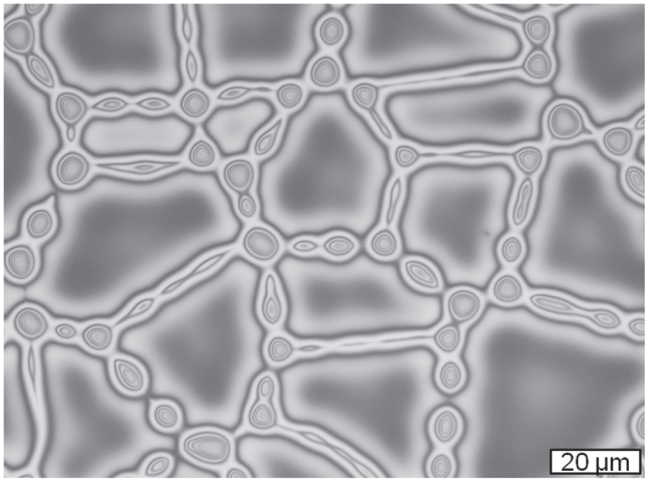

Figure 2. Optical microscopy image of a dewetted P4VP-PS bilayer, consisting of droplets and interconnected cylinders of P4VP on a PS background. The micropattern was formed by annealing a P4VP-PS bilayer at 200 °C for 5 min. The original sample consisted of a 35 nm P4VP layer on top of a 95 nm PS layer on silicon, prepared by sequential spin coating (see Experimental Section).

The height of the P4VP droplets was analyzed by tapping mode AFM (**Figure 3**a,b). The average droplet height varied approximately linearly with the initial P4VP layer thickness (Figure 3b), providing access to a range of droplet heights from 0.5 to 2.5 μm. Taller droplets could be created by dewetting thicker top P4VP layers, providing good control over the synthesis of the micropatterns, however the effect of droplet height with respect to atmospheric water capture is yet to be examined. Similarly, the choice of different starting materials yields hydrophilic droplets with differing geometries (height, base diameter, and interfacial contact angle); as an example we also synthesized micropatterned P4VP surfaces on a hydrophobic self-assembled monolayer of octadecyltrichlorosilane (OTS).[15] The use of a more hydrophobic background phase (OTS is more hydrophobic than PS) yielded a denser array of smaller P4VP droplets (approx. 1 μm diameter).

The micropatterned surfaces were evaluated with respect to atmospheric water capture relative to flat polymer films, to demonstrate an advantage in creating the microstructure. The dew point (the temperature at which condensation is observed at a particular relative humidity (RH)) at the surface was determined by time-lapse optical microscopy using a temperature-controlled stage with a programmed temperature ramp. **Table 1** presents the data for micropatterned PS-P4VP bilayers, and for flat PS and P4VP films. The measured dew point was lower

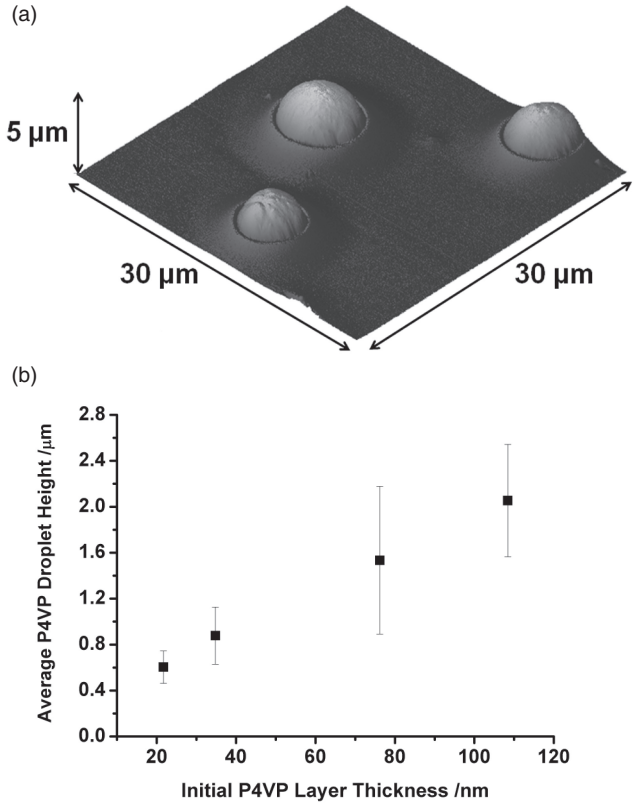

Figure 3. a) 3D topographical image from tapping mode AFM of P4VP droplets on a flat PS background (initial bilayer: 109 nm P4VP layer on top of a 96 nm PS layer). b) Average P4VP droplet height (as measured by tapping mode AFM) as a function of the initial P4VP layer thickness prior to annealing. Approximately ten droplets were measured at each film thickness.

than predicted for all surfaces, but the result for the micropatterned PS-P4VP surface was similar to those of a flat P4VP film, indicating the same ability to facilitate condensation.

The micropatterned surfaces were examined along with flat P4VP and PS films with respect to the volume of condensed water and the rate of condensation on the surface, and a significant improvement in results on patterned PS-P4VP bilayers was observed. Highlighting the thermodynamic aspect of the condensation process, water was observed to first condense on the hydrophilic P4VP bumps and not the PS phase (see video in the Supporting Information). This is identical to the mechanism utilized by the *Stenocara*, where hydrophilic bumps act as "seeding points" for condensation.[2] It is also readily observed that condensed droplets grow and then coalesce, often being pinned by multiple P4VP domains. **Figure 4**a shows the approximate volume of condensed water per unit surface area on different surfaces, as measured by time-lapse microscopy at 0 °C and ≈60% RH in ambient conditions, i.e., in absence of moving air (see Supporting Information for the method used). Surface condensation can occur at any condition below the dew point, however these conditions were chosen so that a significant amount of condensation could be observed. The "ambient" condensation rate was approximately 45% greater on a micropatterned PS-P4VP surface than on a flat P4VP film, and much greater (≈82%) compared to a flat PS film. Approximately the same enhancement effect was seen when micropatterned P4VP-OTS surfaces were prepared (data not shown).

To simulate real-world conditions such as wind, we tested the micropatterned surfaces under a stream of humidified air. Two different flow rates (1.4 and 9.8 L min^{-1}) of humidified air (RH ≈ 80–85%) were used, with surfaces mounted on a temperature-controlled cold stage at 0°C. The mass of water collected was used to determine dynamic rates of condensation. There was a significant enhancement in the amount of water collected on the micropatterned PS-P4VP surfaces relative to both flat P4VP and PS films (Figure 4b). The condensation rate on the patterned surfaces was measured to be 3.4 ± 0.2 L m^{-2} h^{-1} under conditions of high flow rate, which represented a realistic wind speed of approximately 10 km h^{-1}. According to our knowledge, this is the first reported example of water collection directly from humid air, as opposed to previous examples,[6b] which have been tested in a mist or fog. This result is exciting, as it demonstrates that it is possible to collect a significant volume of water directly from the atmosphere using surfaces prepared spontaneously with minimal specialized equipment.

Micropatterned surfaces also facilitate easier detachment of water droplets from the surface when compared to flat hydrophilic films. Static (θ_{eq}) and dynamic (advancing θ_{adv} and receding θ_{rec}) contact angles of water on all surfaces are given in **Table 2**, together with predictions for the critical droplet volume V_{crit} (see Supporting Information). The equilibrium contact angle for dewetted PS-P4VP films was similar to that of PS (θ_{eq} = 90.2° ± 1.9°), but dynamic contact angle values were intermediate between those of PS and those of P4VP. Droplet detachment on smooth films is governed mainly by contact angle hysteresis,[16] with detachment occurring when the force

Table 1. Measured and predicted dew point data for surfaces considered in this work. The measurements were taken by time lapse optical microscopy on a temperature-controlled stage.

Film	Surrounding Air Temperature [°C]	Relative Humidity [%]	Dew Point (measured) [°C]	Dew Point (predicted) [°C][a)]	–Difference [°C]
PS	18.2	66.1	7.8 ± 0.1	11.7 ± 0.2	3.9 ± 0.2
P4VP	20.1	56.9	9.6 ± 0.1	11.2 ± 0.3	1.6 ± 0.3
Dewetted PS-P4VP bilayer	20.1	54.4	9.1 ± 0.1	10.6 ± 0.3	1.5 ± 0.3

[a)]Predicted dew points are found from the temperature and relative humidity of the surrounding air using the August–Roche–Magnus approximation for the saturation vapor pressure of water in air as a function of temperature.[18]

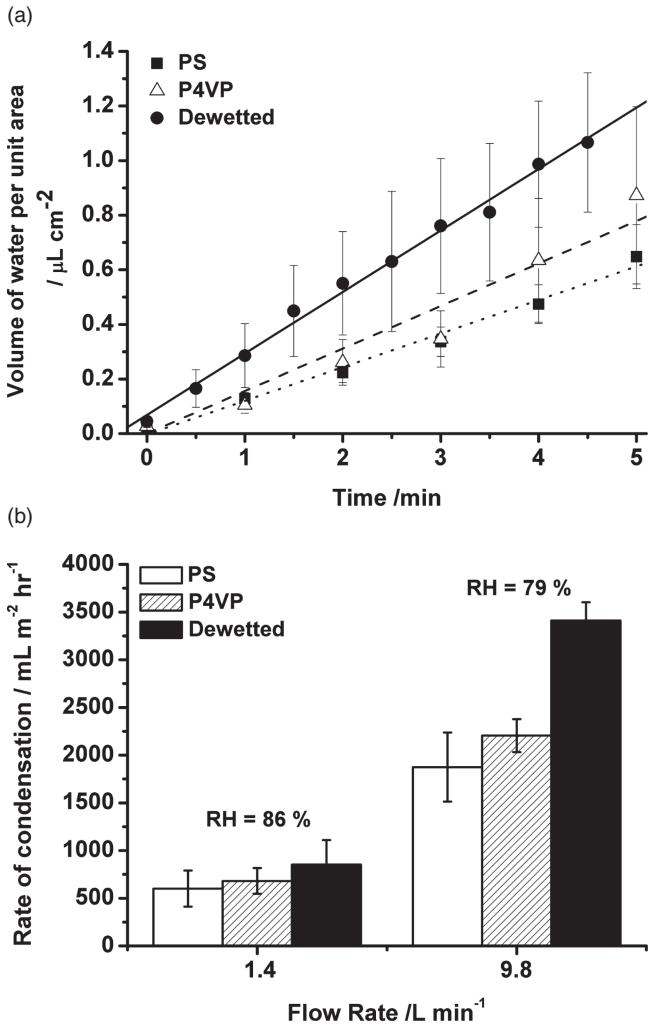

Figure 4. a) Amount of water collected (volume per unit area) as a function of time as observed by time-lapse microscopy at 0°C (RH ≈ 60%) for flat and micropatterned dewetted films. b) Rate of condensation (mL m^{-2} h^{-1}) measured on flat and micropatterned dewetted surfaces held at 0 °C under a flow of humidified air. The micropatterned surface used in these experiments was prepared by dewetting at 200 °C for 30 min a P4VP-PS bilayer consisting of a 45 nm P4VP layer on top of a 96 nm PS layer.

on the right hand side of Equation 2 exceeds that on the left hand side:

$$w(V)\,\gamma(\cos\theta_{rec} - \cos\theta_{adv}) = \rho g\, V \sin\alpha \quad (2)$$

where α is the substrate tilt angle, w and V the width (diameter at the interface) and volume of the droplet, respectively, and γ, ρ, and g the surface tension of water, density of water, and acceleration due to gravity, respectively. A smaller hysteresis allows for droplet roll-off at lower tilt angles of the substrate.

The contact angle hysteresis decreased from approximately 33° on flat P4VP films to ≈23° on the micropatterned surfaces studied in this work. Because of this reduction, water droplets detached from micropatterned substrates at lower volumes

Table 2. Static and dynamic contact angle data for water on surfaces used in this study. Dynamic contact angle data was used to predict the critical droplet volume V_{crit} for detachment from a substrate (see Supporting Information) for comparison to experimental data.

Film	θ_{eq} [°]	θ_{adv} [°]	θ_{rec} [°]	V_{crit} [predicted, μL]	V_{crit} [measured, μL][a)]
PS	91.3 ± 1.8	92.1 ± 1.7	79.4 ± 3.7	3.3	10
P4VP	36.0 ± 2.7	58.6 ± 1.8	25.8 ± 2.0	29.9	n/a [b)]
Dewetted PS-P4VP bilayer	90.2 ± 1.9	93.7 ± 1.6	70.3 ± 1.1	12.7	15

[a)]Data in this column represents the droplet volume where detachment occurred prior to a tilt angle less than 90 °. Data was collected in 5 μL increments; [b)]No droplet roll-off was measured for this sample, up to the largest droplet size measurable by goniometry (35 μL).

(>15 μL) than for flat P4VP films (no droplet detachment was seen for water droplets ranging from 0–30 μL). Flat PS films have the lowest hysteresis of the three films considered, however they condense the least amount of water. The tilt angle for droplet detachment was measured as a function of droplet volume on a tilting-stage contact angle goniometer (see Supporting Information), with tilt angles slightly higher than those predicted for flat featureless films, which was attributed to the "pinning" effect of the raised hydrophilic bumps. We note that a macroscopic droplet that can successfully detach from the micropatterned surfaces would be pinned by many thousands of P4VP domains on the basis of size; this is quite different from *Stenocara*, where droplets detach from individual hydrophilic domains and then roll across the hydrophobic phase. We interpret these results as a demonstration of the importance of surface micropatterning for water collection; the hydrophilic bumps serve as sites for rapid condensation, while the background phase ensures that a macroscopic water droplet has a lower contact angle hysteresis than on a flat hydrophilic film. This ease of droplet detachment (relative to flat films) minimizes re-evaporation and makes water collection easier if the surfaces were eventually mounted on a tilted substrate, such as the roof of a building.

Significant improvements could be made to the fabrication of substrates for atmospheric water capture by polymer film dewetting, such as the choice of materials for each phase, as well as the size and density of hydrophilic spots. For example, it has been shown[6b] that changing the spot size and density significantly changes the volume of water collected. Attempts to model the microstructure (surface topography and spot density) that optimize the water capture process on these substrate are currently underway. Additionally we plan to investigate surface water capture on large-scale samples (up to 1 m^2), which could be prepared by dip coating, in order to examine the applicability of these surfaces in a real-world setting. Irrespective of this, the results presented here already demonstrate a facile and scalable methodology to create surface coatings that capture significant volumes of water using low-cost materials and requiring only the cooling of the surface below the dew point. In many urban environments, water could be collected on these surfaces at night, taking advantage of radiative cooling of the substrate

surface, providing a new method of localized and sustainable water collection.

Experimental Section

Experiments were performed on polymer bilayer films cast onto polished, prime grade silicon wafers (MMRC Pty Ltd, Australia) that were cleaned by standard procedures[10b,17] followed by sonication in distilled ethanol and acetone and finally blown dry with high-purity nitrogen. Bilayer films were prepared by sequential spin coating, firstly PS (number average molecular weight 96 kg mol^{-1}, polydispersity index 1.04, Polymer Standards Service, Mainz, Germany) from a toluene solution at a concentration of 20 mg mL^{-1}, followed by a layer of P4VP (number average molecular weight 19 kg mol^{-1}, polydispersity index 1.15, Polymer Source, Montréal, Canada) from ethanol solutions ranging in concentration from 5–20 mg mL^{-1}. Typical spin speeds were 3000–5000 rpm; the thickness of the PS layer was 96.8 nm ± 0.4 nm, while the P4VP layer was varied from 10–150 nm (measured by ellipsometry; J.A. Woollam Co. Inc., model M-2000V at an angle of incidence of 75°).

Thin film annealing took place at temperatures >160 °C (above the bulk T_g values for both polymers) on a temperature-controlled hot plate (ATV TR-124, Munich, Germany) in air. Thin film characterization and monitoring of the dewetting process was performed by optical microscopy (Nikon LV-150 optical microscope in reflectance mode) and tapping-mode atomic force microscopy (Multimode Nanoscope III, Veeco, Santa Barbara, using silicon AFM tips with a force constant of 40 N m^{-1}). Static and dynamic contact angle measurements, as well as sliding angle measurements, were performed using a KSV CAM200 goniometer (Helsinki, Finland) using a custom-built tilting stage. Dynamic contact angle measurements were taken by dispensing and withdrawing water droplets of approximate volume 5 µL at a rate of 0.1 µL s^{-1}. The equilibrium, advancing, and receding contact angle of water on the films were measured at three different locations on at least three different samples, and the average and standard deviation of these values were calculated. Static and dynamic condensation experiments were carried out via a combination of time-lapse optical microscopy coupled to a temperature-controlled cooling stage (Linkam Instruments, UK), as well as a Peltier cooling stage (CP-031, TE Technology, MI, USA) with an adjustable tilt angle set to 0 °C, mounted in a custom-built chamber to allow for a flow of turbulent humidified air.

Supporting Information

Supporting Information is available from the Wiley Online Library or from the author.

Acknowledgements

This work was funded by the Institute for Sustainable Solutions at The University of Sydney. The authors acknowledge the assistance of the Australian Microscopy & Microanalysis Research Facility at The University of Sydney.

Received: January 24, 2011
Revised: April 19, 2011
Published online: July 15, 2011

[1] FogQuest: Sustainable Water Solutions, http://www.fogquest.org, (accessed August 2010).
[2] A. R. Parker, C. R. Lawrence, *Nature* **2001**, *414*, 33.
[3] a) G. Reiter, *Phys. Rev. Lett* **2001**, *87*, 1861011; b) G. Reiter, M. Hamieh, P. Damman, S. Sclavons, S. Gabriele, T. Vilmin, E. Raphael, *Nat. Mater.* **2005**, *4*, 754; c) P. G. de Gennes, *Rev. Mod. Phys.* **1985**, *57*, 827; d) G. Reiter, *Phys. Rev. Lett.* **1992**, *68*, 75.
[4] J. R. Henschel, M. K. Seely, *Atmos. Res.* **2008**, *87*, 362.
[5] K. K. Varanasi, M. Hsu, N. Bhate, W. Yang, T. Deng, *Appl. Phys. Lett.* **2009**, *95*, 094101.
[6] a) C. Dorrer, J. Ruehe, *Langmuir* **2008**, *24*, 6154; b) R. P. Garrod, L. G. Harris, W. C. E. Schofield, J. McGettrick, L. J. Ward, D. O. H. Teare, J. P. S. Badyal, *Langmuir* **2007**, *23*, 689.
[7] C. Graham, P. Griffith, *Int. J. Heat. Mass. Transfer* **1973**, *16*, 337.
[8] R. Chen, X. Zhang, Z. Su, R. Gong, X. Ge, H. Zhang, C. Wang, *J. Phys. Chem. C* **2009**, *113*, 8350.
[9] L. Zhai, M. C. Berg, F. C. Cebeci, Y. Kim, J. M. Milwid, M. F. Rubner, R. E. Cohen, *Nano Lett.* **2006**, *6*, 1213.
[10] a) C. Neto, K. Jacobs, *Physica A* **2004**, *339*, 66; b) C. Neto, K. Jacobs, R. Seemann, R. Blossey, J. Becker, G. Gruen, *J. Phys.: Condens. Matter* **2003**, *15*, 3355; c) R. Seemann, S. Herminghaus, K. Jacobs, *J. Phys.: Condens. Matter* **2001**, *13*, 4925; d) R. Seemann, S. Herminghaus, C. Neto, S. Schlagowski, D. Podzimek, R. Konrad, H. Mantz, K. Jacobs, *J. Phys.: Condens. Matter* **2005**, *9*, S267; e) L. Léger, J. F. Joanny, *Rep. Prog. Phys.* **1992**, *55*, 431.
[11] P.-G. de Gennes, F. Brochard-Wyart, D. Quéré, *Capillarity and Wetting Phenomena. Drops, Bubbles, Pearls, Waves*, Springer, New York **2004**.
[12] S. C. Thickett, A. Harris, C. Neto, *Langmuir* **2010**, *26*, 15989.
[13] B. Harnish, J. T. Robinson, Z. Pei, O. Ramstrom, M. Yan, *Chem. Mater.* **2005**, *17*, 4092.
[14] A. Sharma, G. Reiter, *J. Colloid Interface Sci.* **1996**, *178*, 383.
[15] J. Sagiv, *J. Am. Chem. Soc* **1980**, *102*, 92.
[16] C. G. L. Furmidge, *J. Colloid Sci* **1962**, *17*, 309.
[17] C. Neto, K. Jacobs, R. Seemann, R. Blossey, J. Becker, G. Grün, *J. Phys.: Condens. Matter* **2003**, *15*, S421.
[18] M. G. Lawrence, *Bull. Am. Meteorol. Soc.* **2005**, *86*, 225.